ISSN 1063-7788, Physics of Atomic Nuclei, 2022, Vol. 85, No. 3, pp. 275–281. © Pleiades Publishing, Ltd., 2022.

NUCLEI
Theory

An Investigation on Decay Modes and Half-Life of Nobelium Isotopes

T. Bayram[1)*] and A. Hayder[1)]

Received December 3, 2021; revised December 19, 2021; accepted December 22, 2021

Abstract—Relativistic Mean Field (RMF) theory with density-dependent forces (DD-ME2 and DD-PC1) was utilized to investigate decay modes and half-life of superheavy $^{247-266}$No isotopes. Triaxially deformed RMF model was used to obtain potential energy surfaces (PESs) of the considered nuclei which is used to determine their ground-state (g.s.) shape. By regarding PES results, axially deformed RMF calculations have been employed to obtain g.s. binding energy (BE) of $^{247-266}$No nuclei. The calculated g.s. BE values of the nobelium isotopes have been used for the prediction of α, β^+/EC, β^- and spontaneous fission (SF) decay modes and half-life of $^{247-266}$No isotopes. Our results show that the $^{247-266}$No isotopes are well deformed and their shapes are predicted to be prolate. According to existing experimental data, our estimates for decay modes and half-lives are in agreement.

DOI: 10.1134/S1063778822030048

1. INTRODUCTION

Investigation of superheavy nuclei (SHN) beyond Fermium ($Z = 100$) has received much attention because of the success of syntheses of SHN in labs during the last four decades [1–10]. The emergence of cold fusion reactions, which are primarily performed at GSI, [1–3] and hot fusion and/or actinide-based fusion reactions, which are primarily performed at JINR, [4–6, 8] has inspired research on SHN. The decay of nuclei is an important tool to investigate the structure of light, medium, and heavy nuclei, as well as SHN produced at the accelerator centers around the world [7, 10–13]. When SHN are produced in the laboratory, they transit from the excited state to the ground state (g.s.) through the decay chains. The observation of these particles is used for getting information about the identification of the new synthesized SHN. These also offer promising potential for learning more about these SHN's nuclear characteristics.

Generally, the super-heavy nuclei are synthesized by a beam of heavy-ions brought into the target nucleus. The nuclei with $Z = 108$, 110, 111, 112 are synthesized by cold fusion reactions. The nuclei synthesized from this reaction have short half-life. On the other hand the hot fusion reactions are used to synthesize the $Z = 112$, 114, 116, 118 nuclei [14]. The nuclei synthesized from hot fusion reactions have relatively long half-life compared to those synthesized by cold fusion reaction. This difference in half-lives is due to the variance in neutrons' number of compound nuclei resulting from cold and hot reactions [15]. Significant information could be obtained from studying the fission of super-heavy nuclei, such as cross section of compound nuclei, the fission barriers and survival probabilities of these nuclei [16]. The decay mode and newly synthesized SHN stability are currently receiving a lot of interest. The SF and α-decay processes are primarily responsible for the transformation of SHN with atomic number $100 \leq Z \leq 118$ [1, 2, 6–8]. It is worth mentioning that other less preferred potential β-decay modes for SHN that occurred by the weak interaction also exist [9, 17].

In order to produce and investigate SHN in the laboratory, the properties of radioactive decay must be theoretically known. Accordingly, understanding SHN decay modes and half-lives by the use of advanced theories is critical for SHN synthesis and experimental advancement in the future [18]. The RMF theory is concidered to be very powerfull in investigating various finite nuclei properties. These finite nuclei could be on stability line or away from it in the nuclidic chart [19–32]. In the present work, the RMF theory together with the phenomenological formula are used to investigate the α, β^+/EC, β^- and SF decay modes and half-life of $^{247-266}$No isotopes.

The sections of this paper are organized in the following order: In Section 2, the RMF formalism and formula for estimation of α, $\beta^{\pm}$, EC, and SF decay half-livies are given briefly. The third section contains

[1)]Department of Physics, Karadeniz Technical University, Trabzon, Turkey.
[*]E-mail: t.bayram@ymail.com

the study results and discussion. Finally, in Section 4, we present our conclusions.

2. THEORETICAL FRAMEWORK AND DETAILS OF CALCULATIONS

The purpose of this section is the discussion of theoretical approaches employed in this study, and it is sub-divided into three parts. The RMF formalism, that is used in the calculation of the ground-state BEs of $^{247-266}$No, is discussed in the first part. In the second part, we discuss approaches to estimate α and SF decay half-life. In the third part, approaches for the estimation of $\beta^{\pm}$ and EC-decay half-lives are given.

2.1. RMF Theory

The nucleons are thought to oscillate in an independent manner in the mean field produced by the exchange of mesons and photons in the RMF theory [19–24]. The Lagrangian is invariant under parity transformation and, since only the solutions with defined parity are considered, the expectation value of the pseudoscalar pion field vanishes in the Hartree approximation. In the present study, only σ, ω and ρ mesons are considered. Based on handling of self-interaction of mesons and density-dependent meson–nucleon couplings, a few types of non-linear RMF model versions could be found (For more details and references see [25]). This subsection briefly describes the RMF model-based density-dependent meson–nucleon couplings. The RMF model begins with the phenomenological relativistic Lagrangian density, which is given as

$$\begin{aligned} L = \bar{\Psi}(i\gamma\partial - m)\Psi + \frac{1}{2}(\partial\sigma)^2 - \frac{1}{2}m_\sigma\sigma^2 \quad (1)\\ - \frac{1}{4}\mathbf{\Omega}_{\mu\nu}\mathbf{\Omega}^{\mu\nu} + \frac{1}{2}m_\omega^2\omega^2 - \frac{1}{4}\overrightarrow{\mathbf{R}}_{\mu\nu}\overrightarrow{\mathbf{R}}^{\mu\nu} + \frac{1}{2}m_\rho^2\overrightarrow{\rho}^2\\ - \frac{1}{4}\mathbf{F}_{\mu\nu}\mathbf{F}^{\mu\nu} - g_\sigma\bar{\Psi}\sigma\Psi\\ - g_\omega\bar{\Psi}\gamma.\omega\Psi - g_\rho\bar{\Psi}\gamma.\vec{\rho}\vec{\tau}\Psi - e\bar{\Psi}\gamma.A\frac{1-\tau_3}{2}\Psi. \end{aligned}$$

where m, m_σ, m_ω, m_ρ are the mass of nucleon, σ, ω and ρ mesons, respectively. The g_σ, g_ω and g_ρ are the coupling constants of the mesons. The interaction strengths of nucleons with meson fields are represented by these coupling constants. Vector field tensors in this equation are given as,

$$\begin{aligned} \mathbf{\Omega}^{\mu\nu} &= \partial^\mu\omega^\nu - \partial^\nu\omega^\mu, \quad (2)\\ \overrightarrow{\mathbf{R}}^{\mu\nu} &= \partial^\mu\overrightarrow{\rho}^\nu - \partial^\nu\overrightarrow{\rho}^\mu,\\ \mathbf{F}^{\mu\nu} &= \partial^\mu A^\nu - \partial^\nu A^\mu. \end{aligned}$$

where the photon field, A^μ, is related with electromagnetic interaction due to protons. In Eq. (1), vectors in three-dimensional space are shown in bold symbols while vectors in isospin space are marked with arrows above them. The unknown meson masses and coupling constants are fitted by using a few experimental data. The meson–nucleon vertex functions can be fixed-on by tuning the parameters of the assumed phenomenological density dependence of the meson–nucleon couplings to regenerate the properties of symmetric and asymmetric nuclear matter and finite nuclei (for details see [26]).

By applying the classical variational principle to the relativistic Lagrangian density given in Eq. (1) the RMF equations can be obtained. The coupled equations that are obtained are Dirac equation with the potential terms for the nucleons and the Klein–Gordon-like equations with sources for mesons and photon. The wave functions can be extended in terms of a spherical, axially, and triaxially symmetric harmonic oscillator potential to solve each of these equations individually [33]. In this study, we used axially and triaxially symmetric RMF calculations to produce ground-state BE of $^{247-266}$No isotopes taking into account the recipe from [33]. First, the triaxially deformed calculations have been performed to get potential energy surfaces (PESs) of the considered isotopes. The obtained PESs have been analyzed to predict the ground-state shape of $^{247-266}$No isotopes (oblate or prolate). Later, the axially deformed RMF calculations have been implemented to determine g.s. BE of the considered nuclei. Two forms of density-dependent RMF interactions, DD-ME2 [26] and DD-PC1 [34], were used in our calculations.

2.2. α-Decay and Spontaneous Fission Decay

The Q-value (released energy) for the α-decay can be otained from mass excesses or total BE of nuclei by using the following formula [35].

$$\begin{aligned} Q_\alpha(Z,A) &= M(Z,A) - M(Z-2,A-4) \quad (3)\\ &- M(2,4) = \mathrm{BE}(Z-2,A-4)\\ &+ \mathrm{BE}(2,4) - \mathrm{BE}(Z,A). \end{aligned}$$

The mass excess $M(2,4)$ and binding energy BE(2, 4) of ^{4}He are 2.42 and 28.30 MeV, respectively. The $\log T_\alpha$ value of α-decay (in units of second) can be estimated by using recently modified Royer formula [36]:

$$\begin{aligned} \log_{10} T_\alpha\,(\mathrm{s}) &= \alpha + bA^{1/6}\sqrt{Z} \quad (4)\\ &+ \frac{cZ}{\sqrt{Q}} + dI + eI^2, \end{aligned}$$

where $I = \dfrac{(N-Z)}{A}$ and the constant parameters a, b, c, d and e in the above Eq. (4) are obtained from [36].

The half-lives for SF decay are estimated by using the recipe of Karpov et al. [37]. The half-lives for SF decay are dependent on three parameters which are the fission barrier heights B_f, the fissility parameter Z^2/A, and the even–odd corrections. The formula used in this work is given below. In this equation, the B_f is estimated as a sum of the liquid-drop barrier B_f (LDM) which is obtained from [38] and the ground state shell correction δU (g.s.) [37].

$$\log_{10} T_{\mathrm{SF}} = 1146.44 - 75.3153\frac{Z^2}{A} \quad (5)$$
$$+ 1.63792\left(\frac{Z^2}{A}\right)^2 - 0.0119827\left(\frac{Z^2}{A}\right)^3$$
$$+ B_f\left(7.23613 - 0.0947022Z^2/A\right)$$
$$+ \begin{cases} 0, & Z \text{ and } N \text{ are even,} \\ 1.53897, & A \text{ is odd,} \\ 0.80822, & Z \text{ and } N \text{ are odd.} \end{cases}$$

2.3. $\beta^{\pm}$-Decay and Electron Capture

The Q-values (released energy) for the β^-, β^+ and EC can be otained from mass excess $M(Z,A)$ or total binding energy of nuclei $\mathrm{BE}(Z,A)$ as indicated in the following Eq. (6), Eq. (7) and Eq. (8), respectively.

$$Q_{\beta^-} = M(Z,A) - M(Z+1,A) \quad (6)$$
$$= \mathrm{BE}(Z+1,A) + \mathrm{BE}(Z,A) + M_n - M_H.$$

$$Q_{\beta^+} = M(Z,A) - M(Z-1,A) - 2m_0c^2 \quad (7)$$
$$= \mathrm{BE}(Z-1,A) + \mathrm{BE}(Z,A)$$
$$+ M_n - M_H - 2m_0c^2.$$

$$Q_{\mathrm{EC}} = M(Z,A) - M(Z-1,A) \quad (8)$$
$$- \mathrm{BE}(\text{electron}) = \mathrm{BE}(Z-1,A) + \mathrm{BE}(Z,A)$$
$$+ M_n - M_H - \mathrm{BE}(\text{electron}).$$

In this work, for the investigation of the probability of $\beta^{\pm}$-decay and EC we followed Fiset and Nix [39]. The inverse half-lives for $\beta^{\pm}$-decay and EC to the g.s. of the daughter nuclei are given in Eq. (9) and Eq. (10), respectively.

$$T_{\beta} = \frac{540m_0^5}{\rho\left(W_{\beta}^6 - m_e^6\right)} \times 10^{5.0}s, \quad (9)$$

W_{β} and m_e are the total energy $Q_{\beta} + m_e$ for emitted β-particles and electron's rest mass energy sequently. ρ is the density of nuclear states taken to $e^{-A/290}\times$ number of states within 1 MeV of ground state for the daughter nucleus, are utilized from [40] results.

$$T_{\mathrm{EC}} = \frac{9m_e^2}{2\pi\left(\alpha Z_K\right)^{2s+1}\rho\left[Q_{\mathrm{EC}} - (1-s)\,m_e\right]^3} \quad (10)$$
$$\times \left(\frac{2R_0}{\frac{\hbar c}{m_e}}\right)^{2-2s} \frac{\Gamma(2s+1)}{1+s} \times 10^{6.5}s.$$

In Eq. (10), Z_K is the parent nucleus' effective charge for an electron in the K-shell, which can be written as $Z_K = Z_P - 0.35$ where Z_P is the proton number of parent nucleus. α and R_0 are the fine structure and nuclear radius, respectively.

3. RESULTS AND DISCUSSION

The deformation of nuclei is one of the most essential nuclear properties. Previous studies predicted that superheavy nuclei are well deformed except superheavy nuclei which have shell closure [28, 41]. In the present study, we were first interested in the prediction for ground-state shape of $^{247-266}$No isotopes. For triaxial shapes with both gamma and beta deformations, we used restricted self-consistent RMF + BCS computations with DD-PC1 and DD-ME2 interactions. In our computations that are based on both DD-PC1 and DD-ME2 equations, prolate shape configuration for all considered nobelium isotopes were predicted. The calculated quadrupole deformation parameters of $^{247-266}$No isotopes with DD-PC1 and DD-ME2 interactions have been found to be between $\beta_2 = 0.24$ and $\beta_2 = 0.29$. We have employed self-consistent axially deformed RMF model calculations by regarding prolate configuration of superheavy $^{247-266}$No isotopes to obtain their g.s. binding energies. The calculated g.s. BE of $^{247-266}$No nuclei obtained by using density-dependent DD-PC1 and DD-ME2 interactions are presented in Fig. 1. In addition, the RMF model calculation outcomes with non-linear NL3* interaction [28], Hartree–Fock–Bogoliubov (HFB) method with SLy4 parameter set [42], Finite Range Droplet Model (FRDM) [43] and available experimental data [44] are also demonstrated in Fig. 1 for comparision. As it can be seen in the figure, RMF model results obtained by using DD-PC1 and DD-ME2 functionals and the predictions of FRDM model for g.s. BE of $^{247-266}$No nuclei are in great harmony with experimental data rather than the results of HFB method with SLy4 parameter set and RMF model with NL3* interaction. It should be noted that the RMF model with density-dependent forces which have small number of adjusted parameters predicts g.s. BE of $^{247-266}$No isotopes as efficient as FRDM

Table 1. Root mean square error (RMSE) of α, β^- and β^+/EC-decay Q values for nobelium isotopes

Nuclei	Q_α, MeV			Q_{β^-}, MeV		
	FRMD	RMF-PC1	RMF-ME2	FRMD	RMF-PC1	RMF-ME2
$^{247-266}$No	0.083	0.156	0.238	0.143	0.476	0.613
Nuclei	Q_{β^+}, MeV			Q_{EC}, (MeV)		
	FRMD	RMF-PC1	RMF-ME2	FRMD	RMF-PC1	RMF-ME2
$^{247-266}$No	0.140	0.136	0.373	0.145	0.154	0.202

Table 2. Comparison of decay modes and half-lives obtained from RMF model with density-dependent PC1 interactions for nobelium isotopes; experimental decay modes and half-lives are taken from [45]

Nuclei	$\log T_{1/2}$					Decay mode		$T_{1/2}$	
	$\log T_\alpha$	$\log T_{\beta^-}$	$\log T_{\beta^+}$	$\log T_{\mathrm{EC}}$	$\log T_{\mathrm{SF}}$	predicted	expt.	predicted	expt.
^{247}No	19.61	0.81	1.36	2.19	2.28	β^-	–	6.4 s	–
^{248}No	0.18	1.46	2.08	2.79	1.86	α	SF	1.5 s	2 μs
^{249}No	1.60	1.14	1.85	2.42	4.90	$\beta^-/\alpha/\beta^+$	–	13.8 s	–
^{250}No	2.01	1.87	2.92	3.18	4.38	β^-	α/SF	1.2 min	$(4.2 \pm 1.20.9)$ μs
^{251}No	2.17	1.80	2.87	2.88	7.61	β^-	α/SF	1.1 min	(0.80 ± 0.01) s
^{252}No	1.31	2.66	3.86	3.59	7.22	α	α/SF/ε	20.4 s	(2.44 ± 0.04) s
^{253}No	2.44	2.53	4.02	3.37	10.52	α/β^-	α/ε	4.5 min	(1.62 ± 0.15) min
^{254}No	2.76	3.51	5.63	4.30	8.74	α	α/ε/SF	9.5 min	(51 ± 10) s
^{255}No	3.43	3.79	6.26	4.17	9.34	α/β^-	ε/α	44.8 min	(3.52 ± 0.21) min
^{256}No	2.87	4.85	–	5.27	6.65	α	α/SF	12.3 min	(2.91 ± 0.05) s
^{257}No	4.48	5.14	–	5.84	7.10	α	α/ε/SF	8.3 h	(24.5 ± 0.5) s
^{258}No	4.52	6.90	–	–	4.06	SF/α	SF	3.1 h	(1.2 ± 0.2) ms
^{259}No	5.82	–	6.19	–	6.00	α	α/ε/SF	7.6 h	(58 ± 5) min
^{260}No	6.34	–	5.71	–	4.57	SF	SF	10.3 h	(106 ± 8) ms
^{261}No	8.05	–	4.56	–	7.60	β^+	–	10.0 h	–
^{262}No	8.75	7.06	4.55	–	5.90	β^+	SF	9.8 h	5 ms
^{263}No	10.51	5.39	3.64	–	8.33	β^+	–	1.2 h	–
^{264}No	10.94	5.18	2.93	–	7.52	β^+	–	14.1 min	–
^{265}No	8.12	2.96	2.41	–	9.58	β^+/β^-	–	4.2 min	–
^{266}No	5.10	3.40	2.85	–	7.06	β^+	–	11.7 min	–

which is known to be the best model for the prediction of BE through nuclidic chart.

The g.s. BE of Nobelium isotopes that was calculated by using RMF and predicted from FRDM have been used in Eqs. (5), (6), (7) and (8) for calculation Q values for α, β^-, β^+ and EC-decays. The calculted root mean square error (RMSE) values of α, β^-, β^+ and EC-decay Q values for nobelium isotopes by using current experimental data are listed in Table 1. As the figure demonstrates, generally small RMSE values are seen and RMF model outcomes with DD-PC1 interaction seem better than those of DD-ME2 interaction. To validate our calculation results, we have also computed the variation

Table 3. The same as Table 2 but for density-dependent ME2 interaction

Nuclei	$\log T_{1/2}$					Decay mode		$T_{1/2}$	
	$\log T_\alpha$	$\log T_{\beta^-}$	$\log T_{\beta^+}$	$\log T_{\mathrm{EC}}$	$\log T_{\mathrm{SF}}$	predicted	expt.	predicted	expt.
^{247}No	20.22	0.94	1.55		2.28	β^-	–	8.7 s	–
^{248}No	0.97	1.60	2.28	2.89	1.86	α	SF	9.3 s	2 μs
^{249}No	2.61	1.29	2.05	2.51	4.90	β^-	–	19.4 s	–
^{250}No	3.40	2.01	3.43	3.40	4.38	β^-	α/SF	1.7 min	$(4.2 \pm 1.20.9)$ μs
^{251}No	2.99	2.17	3.45	3.13	7.61	β^-	α/SF	2.4 min	(0.80 ± 0.01) s
^{252}No	1.56	3.08	4.61	3.90	7.22	α	α/SF/ε	36.3 s	(2.44 ± 0.04) s
^{253}No	2.88	3.06	5.05	3.77	10.52	$\alpha/\varepsilon/\beta^+$	α/ε	12.6 min	(1.62 ± 0.15) min
^{254}No	3.30	4.15	–	4.94	8.74	α	α/ε/SF	33.2 min	(51 ± 10) s
^{255}No	4.12	4.77	–	5.06	9.34	α	ε/α	3.6 h	(3.52 ± 0.21) min
^{256}No	4.29	6.06	–	6.88	6.65	α	α/SF	5.4 h	(2.91 ± 0.05)s
^{257}No	5.90	7.12	–	–	7.10	α	α/ε/SF	9.2 h	(24.5 ± 0.5) s
^{258}No	6.38	–	6.17	–	4.06	SF	SF	3.2 h	(1.2 ± 0.2) ms
^{259}No	7.90	–	4.75	–	6.00	β^+	α/ε/SF	15.6 min	(58 ± 5) min
^{260}No	8.40	–	4.54	–	4.57	β^+/SF	SF	9.6 min	(106 ± 8) ms
^{261}No	9.76	5.55	3.57	–	7.60	β^+	–	1 min	–
^{262}No	10.10	5.19	3.71	–	5.90	β^+	SF	1.4 h	5 ms
^{263}No	11.88	4.11	–	2.91	8.33	ε	–	13.5 min	–
^{264}No	12.56	4.16	2.45	–	7.52	ε	–	4.6 min	–
^{265}No	9.74	2.40	1.86	–	9.58	α/β^+	–	1.2 min	–
^{266}No	0.41	2.77	2.33	–	7.06	α	–	2.6 s	–

of our calculated Q values using the DD-PC1 and DD-ME2 functionals with the current experimental data [44]. The calculated Q value differences as a function of mass number (A) are shown in Fig. 2. As it can be understood from this figure, the maximum deviation from experimental data is under the values of 2.5 MeV for β^- decay. The calculated Q value differences for α and β^+/EC-decay is lower than the value of 0.8 MeV. It should be noted that the results of DD-PC1 functional seem to be more appropriate for nobelium isotopes as compared to the DD-ME2 functional.

We have employed the calculated Q values obtained from RMF model with density-dependent forces and the equation given in Section 2 to calculate half-lives of α, $\beta^{\pm}$ and EC-decays using Eqs. (4), (9) and (10), sequently. Likewise, the half-life for SF has been calculated by using Eq. (5). The calculated half-lives for $^{247-266}$No isotopes with DD-PC1 and DD-ME2 functionals are mentioned in Table 2 and 3, respectively. In these tables, we have indicated competence of decay modes and the most possible decay mode for each nobelium isotope. Also, we have compared our predictions for decay modes and half-life of probable decay mode with available experimental data [45] in Table 2 and 3 for validation of our results. Just nuclei with a probability of greater than 50 percent of any given decay mode or equivalent decay modes were considered for this comparison. If the half-lives are quite close to each other, more than one decay option is considered. On the other hand, the lowest half-life is indicated in the second last column. The RMF model together with the phenomenological formulas are able to reproduce experimental decay modes and half-lives for most of the nobelium isotopes. Table 2 and 3 show that the possibility of weak decay in Nobelium isotopes cannot be disregarded. According to our projection, that it was discovered that weak decay has the same likelihood as alpha-decay and SF spontaneous fission in Nobelium isotopes, which is consistent with the results for transfermium isotopes of [9, 17]. Our predictions on the half-life of Nobelium isotopes for weak decay are primitive, and more prediction is necessary by involving the phase space factor and the GT strength distribution.

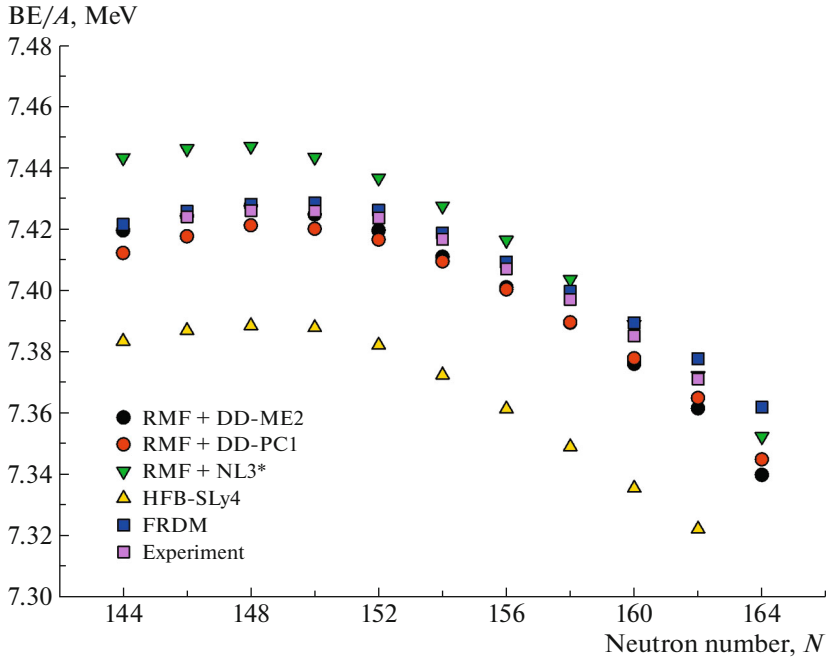


Fig. 1. The calculated and experimental binding energy per nucleon (BE/A) for isotopic chain of even–even No isotopes.

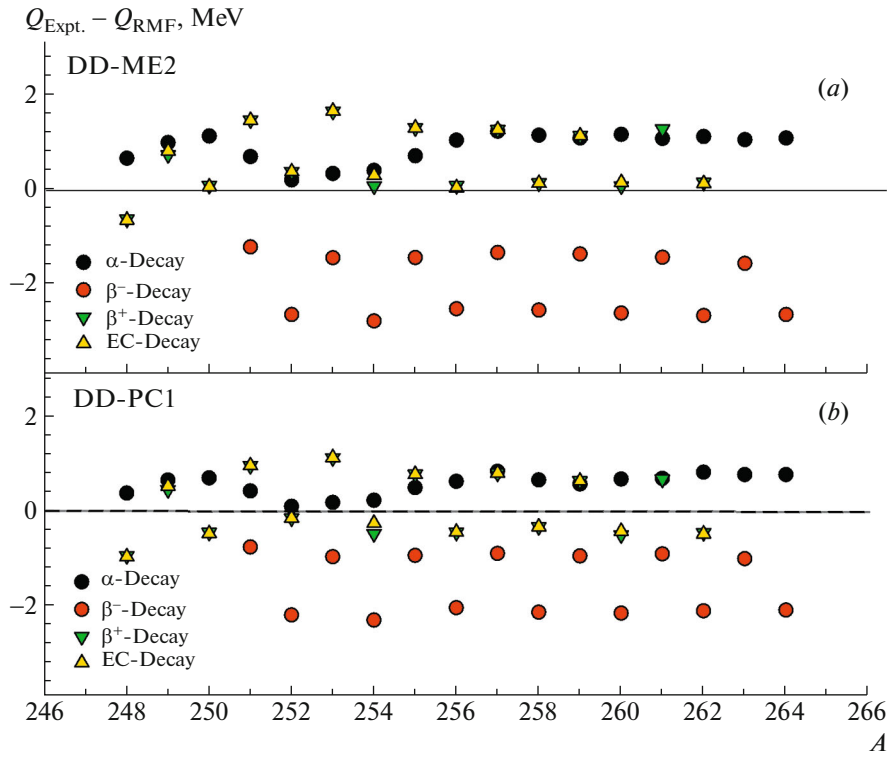


Fig. 2. Difference of calculated and experimental [45] Q values for α, β^- and β^+/EC-decays.

4. CONCLUSIONS

The ground-state shape of $^{247-266}$No nuclei have been investigated by the utilization of the RMF model with density-dependent forces DD-PC1 and DD-ME2. For this purpose, potential energy surfaces of the considered nuclei have been carried out and well deformed prolate shape of the nobelium isotopes in thier g.s. has been reported as in agreement with previous studies. The calculated g.s. binding ener-

gies of $^{247-266}$No isotopes have been found to be in agreement with the available experimental data. The calculated BEs of $^{247-266}$No nuclei have been used to calculate their Q values of α, β^+/EC, β^- and SF-decay modes. By using the calculated Q values, dominant decay modes and half-life of $^{247-266}$No isotopes have been predicted with the help of some empirical formulas. The predictions of the RMF model with density-dependent forces DD-PC1 and DD-ME2 for decay modes and half-lives have been tabulated.

REFERENCES

1. S. Hofmann, V. Ninov, F. P. Heβberger, P. Armbruster, H. Folger, G. Münzenberg, H. J. Schött, A. G. Popeko, A. V. Yeremin, S. Saro, R. Janik, and M. Leino, Z. Phys. A **354**, 229 (1996).
2. S. Hofmann, Rep. Prog. Phys. **61**, 636 (1998).
3. S. Hofmann, Acta Phys. Polon. B **30**, 621 (1999).
4. Yu. Ts. Oganessian, A. V. Yeremin, A. G. Popeko, S. L. Bogomolov, G. V. Buklanov, M. L. Chelnokov, V. I. Chepigin, B. N. Gikal, V. A. Gorshkov, G. G. Gulbekian, M. G. Itkis, A. P. Kabachenko, A. Yu. Lavrentev, O. N. Malyshev, J. Rohac, and R. N. Sagaidak, Nature (London, U.K.) **400**, 242 (1999).
5. Yu. Ts. Oganessian, Rad. Phys. Chem. **61**, 259 (2001).
6. Yu. Ts. Oganessian, Pure Appl. Chem. **78**, 889 (2006).
7. Yu. Ts. Oganessian, J. Phys. G **34**, R165 (2007).
8. Yu. Ts. Oganessian, Nucl. Phys. A **834**, 331c (2010).
9. P.-H. Heenen, J. Skalski, A. Staszczak, and D. Vretenar, Nucl. Phys. A **944**, 415 (2015).
10. Yu. Ts. Oganessian, A. Sobiczewski, and G. M. Ter-Akopian, Phys. Scr. **92**, 023003 (2017).
11. S. Hofmann, F. P. Heβberger, D. Ackermann, G. Münzenberg, S. Antalic, P. Cagarda, B. Kindler, J. Kojouharova, M. Leino, B. Lommel, R. Mann, A. G. Popeko, S. Reshitko, S. Śaro, J. Uusitalo, and A. V. Yeremin, Eur. Phys. J. A **14**, 147 (2002).
12. M. Freer, Rep. Prog. Phys. **70**, 2149 (2007).
13. A. Soylu, Chin. Phys. C **43**, 074102 (2019).
14. A. K. Nasirov, G. G. Adamian, G. Giardina, and A. I. Muminov, in *Proceedings of the 5th International Conference on Modern Problems of Nuclear Physics* (2003), p. 81.
15. V. Zagrebaev and W. Greiner, Phys. Rev. C **78**, 034610 (2008).
16. M. G. Itkis, E. Vardaci, I. M. Itkis, G. N. Knyazheva, and E. M. Kozulin, Nucl. Phys. A **944**, 204 (2015).
17. S. Hofmann, S. Heinz, R. Mann, J. Maurer, G. Münzenberg, S. Antalic, W. Barth, H. G. Burkhard, L. Dahl, K. Eberhardt, R. Grzywacz, J. H. Hamilton, R. A. Henderson, J. M. Kenneally, B. Kindler, and I. Kojouharov, Eur. Phys. J. A **52**, 180 (2016).
18. M. Bhuyan, Phys. At. Nucl. **81**, 15 (2018).
19. J. D. Walecka, Ann. Phys. (N.Y.) **83**, 491 (1974).
20. J. Boguta and A. R. Bodmer, Nucl. Phys. A **292**, 413 (1977).
21. P. Ring, Prog. Theor. Phys. **37**, 193 (1996).
22. G. A. Lalazissis, S. Raman, and P. Ring, At. Data Nucl. Data Tables **71**, 1 (1999).
23. D. Vretenar, A. V. Afanasjev, G. A. Lalazissis, and P. Ring, Phys. Rep. **409**, 101 (2005).
24. Y. K. Gambhir and A. Bhagwat, Phys. Part. Nucl. **37**, 194 (2006).
25. J. Meng, H. Toki, S. G. Zhou, S. Q. Zhang, W. H. Long, and L. S. Geng, Prog. Part. Nucl. Phys. **57**, 470 (2006).
26. G. A. Lalazissis, T. Niksic, D. Vretenar, and P. Ring, Phys. Rev. C **71**, 024312 (2005).
27. A. H. Yilmaz and T. Bayram, J. Korean Phys. Soc. **59**, 3329 (2011).
28. T. Bayram and A. H. Yilmaz, Mod. Phys. Lett. A **28**, 1350068 (2013).
29. T. Bayram and S. Akkoyun, Phys. Scr. **87**, 065201 (2013).
30. T. Bayram, S. Akkoyun, and Ş. Şentürk, Phys. At. Nucl. **81**, 288 (2018).
31. T. Bayram, Phys. At. Nucl. **82**, 317 (2019).
32. J.-U. Nabi, T. Bayram, G. Daraz, A. Kabir, and Ş. Şentürk, Nucl. Phys. A **1015**, 122278 (2021).
33. T. Niksic, N. Paar, D. Vretenar, and P. Ring, Comput. Phys. Commun. **185**, 1808 (2014).
34. T. Niksic, D. Vretenar, and P. Ring, Phys. Rev. C **78**, 034318 (2008).
35. E. L. Medeiros, M. M. N. Rodrigues, S. B. Duarte, and O. A. P. Tavares, J. Phys. G **32**, B23 (2006).
36. D. T. Akrawy and D. N. Poenaru, J. Phys. G **44**, 105105 (2017).
37. A. V. Karpov, V. I. Zagrebaev, Y. Martinez Palenzuela, L. Felipe Ruiz, and W. Greiner, Int. J. Mod. Phys. E **21**, 1250013 (2012).
38. P. Möller, A. J. Sierk, T. Ichikawa, A. Iwamoto, R. Bengtsson, H. Uhrenholt, and S. Aberg, Phys. Rev. C **79**, 064304 (2009).
39. E. O. Fiset and J. R. Nix, Nucl. Phys. A **193**, 647 (1972).
40. P. A. Seeger, W. A. Fowler, and D. D. Clayton, Astrophys. J. Suppl. **11**, 121 (1965).
41. Z. Ren, D. Chen, F. Tai, H. Y. Zhang, and W. Q. Shen, Phys. Rev. C **67**, 064302 (2003).
42. M. V. Stoitsov, J. Dobaczewski, W. Nazarewicz, S. Pittel, and D. J. Dean, Phys. Rev. C **68**, 054312 (2003).
43. P. Möller, A. J. Sierk, T. Ichikawa, and H. Sagawa, At. Data Nucl. Data Tables **109–110**, 1 (2016).
44. M. Wang, G. Audi, F. G. Kondev, W. J. Huang, S. Naimi, and X. Xu, Chin. Phys. C **41**, 030003 (2017).
45. http://www.nndc.bnl.gov/. Accessed on June 14, 2021.